Mon. Not. R. Astron. Soc. **373,** 700–704 (2006) doi:10.1111/j.1365-2966.2006.11057.x

The v_c–σ_c relation in low-mass and low surface brightness galaxies

P. Buyle,[1,2★]† L. Ferrarese,[2] G. Gentile,[3] H. Dejonghe,[1] M. Baes[1] and U. Klein[4]

[1]*Sterrenkundig Observatorium, Universiteit Gent, Krijgslaan 281, S9, B-9000 Ghent, Belgium*
[2]*Herzberg Institute of Astrophysics, National Research Council of Canada, Victoria, BC V9E2E7, Canada*
[3]*University of New Mexico, Department of Physics and Astronomy, 800 Yale Blvd NE, Albuquerque, NM 87131, USA*
[4]*Bonn University, Auf dem Hügel 71D, 53121 Bonn, Germany*

Accepted 2006 September 8. Received 2006 August 22; in original form 2006 March 14

ABSTRACT

We present an updated investigation of the relation between large-scale disc circular velocity, v_c, and bulge velocity dispersion, σ_c. New bulge velocity dispersions are measured for a sample of 11 low surface brightness (LSB) and seven high surface brightness (HSB) spiral galaxies for which v_c is known from published optical or H I rotation curves. We find that, while LSB galaxies appear to define the upper envelope of the region occupied by HSB galaxies (having relatively larger v_c for any given σ_c), the distinction between LSB and HSB galaxies in the v_c–σ_c plane becomes less pronounced for $\sigma_c \lesssim 80$ km s^{-1}. We conclude that either the scatter of the v_c–σ_c relation is a function of v_c (and hence galaxy mass) or the character of the v_c–σ_c relation changes at $v_c \sim 80$ km s^{-1}. Some implications of our findings are discussed.

Key words: black hole physics – galaxies: haloes – galaxies: nuclei – dark matter.

1 INTRODUCTION

The existence of supermassive black holes (SBHs) in galactic nuclei has been accepted since the detections in the nearby spiral NGC 4258 (Miyoshi et al. 1995) and in our own galaxy (Ghez et al. 2003; Schödel et al. 2003). Compelling cases now exist in three dozen additional galaxies (see Ferrarese & Ford 2005 for a review), making it possible to investigate the existence of scaling relations linking the SBH mass, $M_{\rm BH}$, to the overall properties of the host. Indeed, $M_{\rm BH}$ correlates with the blue luminosity $L_{\rm B}$ of the host bulge (Kormendy & Richstone 1995; Marconi & Hunt 2003), with the central light concentration (Graham et al. 2001), and with the bulge velocity dispersion σ_c (Ferrarese & Merritt 2000; Gebhardt et al. 2000). Because of its tight scatter (0.34 dex in $M_{\rm BH}$), the $M_{\rm BH}$–σ_c relation is thought to allow us to peer into the mechanisms controlling the joint formation/evolution of SBHs and galaxies. However, cosmological simulations show that a possibly more fundamental relation should be expected between $M_{\rm BH}$ and the total gravitational mass $M_{\rm tot}$ of the galaxy, or the mass $M_{\rm DM}$ of the dark matter (DM) halo (e.g. Loeb & Rasio 1994; Haehnelt, Natarajan & Rees 1998; Silk & Rees 1998; Cattaneo, Haehnelt & Rees 1999; Adams, Graff & Richstone 2000; Haehnelt & Kauffmann 2000; Monaco, Salucci & Danese 2000; Di Matteo et al. 2003; Kawakatu, Saitoh & Wada 2005; Wyithe & Loeb 2005). Indirect observational evidence for such a link has been found in the form of a correlation between the circular velocity v_c of spirals' discs (obtained by either H I or deep optical observations) and the σ_c of their bulge component (Ferrarese 2002; Baes et al. 2003; Pizzella et al. 2005):

$$\log v_c = (0.84 \pm 0.09) \log \sigma_c + (0.55 \pm 0.29). \qquad (1)$$

Further exploring the v_c–σ_c relation is of interest because, by linking galactic components on vastly different scales, the relation is a reflection of the interplay between discs and spheroids during galaxy formation/evolution. Furthermore, if v_c and σ_c are used as surrogates for $M_{\rm DM}$ and $M_{\rm BH}$ respectively, equation (1) implies a strong causal relation between SBHs and DM haloes.

Pizzella et al. (2005) reported evidence of a separation in the v_c–σ_c plane between high and low surface brightness spiral galaxies (HSB and LSB, respectively), the latter having distinctly larger v_c at a given σ_c compared to the former. Based on this, the authors argue against the importance of baryonic collapse in shaping the density profiles of DM haloes in LSBs, and suggest that for a given DM halo mass, LSBs might host less massive SBHs than HSBs. The behaviour of HSBs themselves is somewhat controversial: while Pizzella et al. (2005) found that HSB in the range $50 \lesssim \sigma_c \lesssim 350$ km s^{-1} (corresponding to $150 \lesssim v_c \lesssim 550$ km s^{-1}) follow a linear relation, Ferrarese (2002) and Baes et al. (2003) claimed that the relation is mildly non-linear for $\sigma_c \gtrsim 80$ km s^{-1} ($v_c \gtrsim 140$ km s^{-1}), and breaks down altogether at lower σ_c, possibly revealing the inability of the least massive haloes to form central SBHs (Loeb & Rasio 1994; Haehnelt et al. 1998; Silk & Rees 1998; Shankar et al. 2006)

The goal of this paper is to investigate the v_c–σ_c relation for a combination of LSB and HSB galaxies, with v_c in the critical range 110–220 km s^{-1}. The data reduction and analysis are discussed in

★E-mail: Pieter.Buyle@UGent.be
†Post-doctoral Fellow of the Fund for Scientific Research – Flanders, Belgium (F.W.O.).

Table 1. Column 1 gives the galaxy's name, while columns 2 and 3 give the J2000 coordinates. The asymptotic circular velocity v_c is tabulated in column 4, it is taken directly from Verheijen (2001) for the HSB galaxies, and measured from the published rotation curves for the LSB galaxies. Central velocity dispersion (σ_c) at $r_e/8$ and the effective radius of the galaxy can be found in columns 5 and 6. The heliocentric radial velocity, Hubble classification, total *I*-band magnitude and inclination can be found in columns 7 to 10 and are taken from Verheijen (2001) for the HSB galaxies and Palunas & Williams (2000) for the LSB galaxies and the online NED data base. Finally, the total exposure time and S/N/pixel at 8500 Å are given in columns 11 and 12.

Name	RA (J2000)	Dec. (J2000)	v_c (km s^{-1})	σ_c (km s^{-1})	r_e (arcsec)	v_{rad} (km s^{-1})	Morph	m_I (mag)	Inclination (°)	Exposure Time (s)	S/N (@ 8500 Å)
					LSB galaxies						
ESO215-G39	$11^h 17^m 04^s$	−49° 12′05″	162±3	71±11	4.5	4335	SABc	12.01	50	500	20.03
ESO268-G44	$12^h 48^m 42^s$	−45° 00′29″	190±9	70±9	3.5	3477	Sb	12.22	62	450	25.68
ESO322-G19	$12^h 29^m 07^s$	−40° 40′24″	141±9	49±10	0	3100	SBc	12.64	79	900	22.19
ESO323-G42	$12^h 55^m 01^s$	−40° 58′20″	158±4	54±9	4	4203	Sc	11.53	69	450	30.32
ESO323-G73	$13^h 04^m 02^s$	−38° 11′57″	163±7	70±7	2	4929	Sbc	12.44	48	450	35.29
ESO374-G03	$09^h 51^m 57^s$	−33° 04′25″	146±3	40±6	6	2931	SABc	11.51	71	600	21.80
ESO382-G06	$13^h 05^m 32^s$	−32° 57′38″	171±4	54±8	2	4809	Sab	13.20	54	600	21.01
ESO444-G21	$13^h 23^m 31^s$	−30° 06′52″	116±21	53±9	4.5	4265	Sc	12.86	84	1900	20.46
ESO444-G47	$13^h 28^m 25^s$	−31° 51′28″	154±6	61±14	0	4389	SBc	12.82	71	900	22.01
ESO509-G91	$13^h 40^m 03^s$	−25° 28′28″	203±9	62±11	6.5	5113	SBc	12.70	79	900	20.91
ESO376-G10	$10^h 42^m 00^s$	−36° 56′07″	220±11	54±12	7	3184	SBd	11.00	76	600	20.27
					HSB galaxies						
NGC 3953	$11^h 53^m 49^s$	+52° 19′36″	223±5	115±9	66	1052	Sbc	9.03	63	2500	60.01
NGC 3877	$11^h 46^m 08^s$	+47° 29′40″	167±11	84±8	53.5	895	Sc	9.91	83	3600	66.08
NGC 4088	$12^h 05^m 34^s$	+50° 32′21″	173±14	62±7	76	757	SABc	9.51	71	3600	58.13
NGC 3949	$11^h 53^m 41^s$	+47° 51′32″	164±7	63±5	36	800	Sbc	10.23	56	4000	57.15
NGC 4157	$12^h 11^m 04^s$	+50° 29′05″	185±10	71±6	35	774	SABb	9.93	90	4000	63.30
NGC 3769	$11^h 37^m 44^s$	+47° 53′35″	122±8	80±7	29	737	Sb	11.08	78	8000	66.25
NGC 3726	$11^h 33^m 21^s$	+47° 01′45″	162±9	63±10	84	866	Sc	9.50	49	6600	38.44

Sections 2 and 3, respectively. Discussion and conclusions can be found in Section 4.

2 OBSERVATIONS AND DATA REDUCTION

To compare the behaviour of LSBs and HSBs in the $v_c \lesssim 220\,\mathrm{km\,s^{-1}}$ range of the v_c–σ_c relation, we drafted a sample of galaxies with v_c known from published rotation curves, and proceeded to obtain new optical spectra from which to measure σ_c. We targeted 11 LSB galaxies with optical rotation curves from the Palunas & Williams (2000) compilation, and seven HSB galaxies with H I rotation curves from the Ursa Major sample of Verheijen (2001). Besides the need of selecting galaxies visible in the given observing season, and bright enough to produce spectra with the required signal-to-noise ratio (S/N), the one essential criterium in our sample selection is that the published rotation curves must be symmetric relative to the galaxy's centre, and reach an asymptotic value at large radii.

Details of the sample and observations are given in Table 1. The LSB galaxies were observed with the VLT/UT4 telescope of the European Southern Observatory on the nights of 2004 April 20, 29 and May 6. The holographic grism GRIS_1028z+29 on FORS2 was centred on the Calcium absorption triplet around 8500 Å, producing an instrumental broadening $\sigma_{\rm instr} \approx 35\,\mathrm{km\,s^{-1}}$ with the 0.7-arcsec slit. The seven HSB galaxies were observed with the TWIN spectrograph at the 3.5-m Calar Alto telescope, on 2005 June 6–19. The T06 grating was used in the first order, again centred at the Ca triplet. The instrumental broadening was $\sigma_{\rm instr} \approx 20\,\mathrm{km\,s^{-1}}$ for the 1.2-arcsec wide slit. All spectra were divided into several exposures to ease cosmic ray identification and removal.

Standard data reduction was performed with MIDAS, IRAF and additional software developed specifically for this project. After basic data processing (dark and bias subtraction, flat-fielding and trimming), atmospheric emission lines were identified and removed through an interpolation scheme, after which the spectra were rectified and wavelength calibrated. Cosmic rays were removed by applying a median filter along the spatial axis.

3 DATA ANALYSIS

Deriving accurate kinematical quantities of galaxies is a non-trivial task. The result of the extraction can vary depending on the applied fitting techniques, the S/N, the template stars, the absorption lines used, etc. (e.g. De Bruyne et al. 2003). To lower this degree of subjectivity, we derived velocity dispersions using two independent techniques: a direct χ^2 fit to the spectrum (De Bruyne et al. 2004), and the PPXF algorithm (Cappellari & Emsellem 2004) (see Fig. 1), which is based on a Penalized Likelihood Approach. Velocity dispersions derived using these two methods agree to within 10 per cent; the final values quoted in Table 1 were obtained using the χ^2 routine. In analysing the spectra, sky residuals that deviated by more than three times the average sigma in the nearby continuum were rejected; furthermore, to minimize the effects of template mismatch, six different template stars were used, each with weight calculated by a quadratic fit to the central row of the spectrum. In keeping with previous works, velocity dispersions were extracted from spectra binned, in the spatial direction, out to one-eighth of the bulge effective radius, estimated from the literature in the case of the HSB galaxies (Courteau 1996; Heraudeau, Simien & Mamon 1996; Baggett, Baggett & Anderson 1998; Möllenhoff & Heidt 2001), and from published surface brightness profiles for the Palunas & Williams (2000) galaxies. Within this radius, the effect of a possible contamination by the disc rotational velocity should be negligible. This was verified by measuring the dispersion profiles along the major axis (without binning spatially); the velocity dispersion of

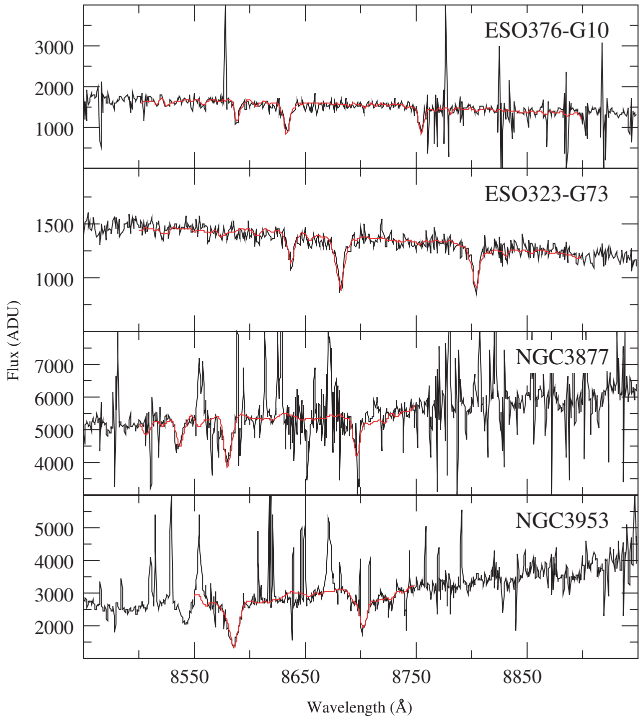

Figure 1. Spectra for four of the programme galaxies are shown in black. The top two panels show spectra obtained at the VLT, while the bottom two panels show Calar Alto spectra. To illustrate the quality of the data, for each telescope we chose to show the two spectra with the lowest (first and third panel from the top) and highest (second and fourth panel from the top) signal-to-noise ratio. The red lines show the best χ^2 fits to each spectrum, overplotted to the real data in the spectral region used to perform the fits. The narrow emission features present in three of the spectra are artefacts resulting from imperfect sky subtraction.

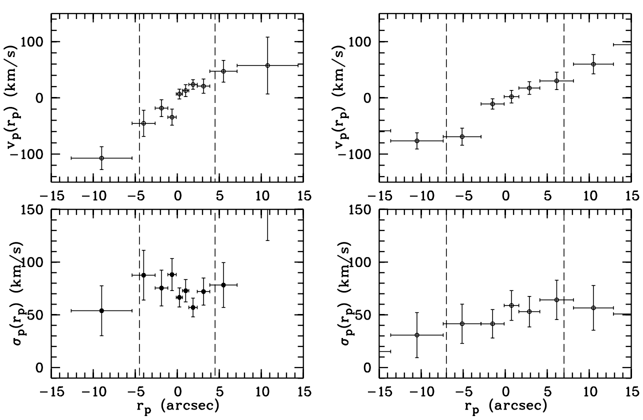

Figure 2. Velocity and velocity dispersion curves for ESO215-G39 (left-hand panel) and ESO376-G10 (right-hand panel) derived by the direct χ^2 method. The vertical dashed lines are drawn at the location of the bulge effective radius, r_e.

most galaxies (see Fig. 2) indeed remained nearly constant in the bulge-dominated region.

The circular rotational velocities and errors are published by Verheijen (2001) for the HSB galaxies. These were derived from H I observations and extend beyond the optical radius (R_{25}), well into the flat part of the curve. For the LSB galaxies, we measured v_c as the weighted average of the flat part of the optical rotation curve published in Palunas & Williams (2000); the error on v_c was derived by means of a bootstrap method and reflects any slight asymmetries in the rotation curves. The optical rotation curves are not as extended as the H I observations of the HSB galaxies; however, all rotation curves reach an asymptotic value at large radii. As shown in Pizzella et al. (2005), when this condition is satisfied, v_c can be extracted reliably; therefore, we do not expect any systematic biases in the v_c measurements between our samples of HSBs and LSBs. The results of the dynamical analysis are given in Table 1.

4 DISCUSSION AND CONCLUSIONS

The v_c–σ_c relation for HSB galaxies is plotted in the left-hand panel of Fig. 3. The 11 LSB galaxies studied in this paper populate the region between $40 \leqslant \sigma_c \leqslant 80$ km s^{-1}, where previously only three galaxies could be found. Furthermore, in the same region, we more than double the number of HSB galaxies, from three to eight. Pizzella et al. (2005) concluded that, relative to the v_c–σ_c relation defined by HSB galaxies, LSB galaxies appear to have larger circular velocities, v_c, at any given value of σ_c. This conclusion is reaffirmed by our data. However, with the addition of the present sample, it has now become more evident that there is some overlap in the locations occupied by LSB and HSB galaxies in the v_c–σ_c plane. In other words, LSB galaxies appear to occupy the *upper envelope* of the strip defined by HSB galaxies. Furthermore, at low-velocity dispersions $30 \leqslant \sigma_c \leqslant 80$ km s^{-1}, the v_c–σ_c relation for both LSB and HSB galaxies appears to be shifted towards larger circular velocities relative to the relation defined by the (HSB) galaxies with larger velocity dispersion.

A least-squares fit, taking into account the errors on both quantities (FITEXY; Press et al. 2002), to the sample of HSBs with $\sigma_c \geqslant 80$ km s^{-1} gives

$$\log v_c = (0.68 \pm 0.04) \log \left(\frac{\sigma_c}{129 \text{ km s}^{-1}} \right) + (2.33 \pm 0.01), \quad (2)$$

with $\chi^2_r = 2.58$. For $30 \leqslant \sigma_c \leqslant 80$ km s^{-1}, on the other hand,

$$\log v_c = (1.33 \pm 0.86) \log \left(\frac{\sigma_c}{63 \text{ km s}^{-1}} \right) + (2.21 \pm 0.03), \quad (3)$$

with $\chi^2_r = 0.23$ for HSB galaxies, and

$$\log v_c = (1.91 \pm 0.68) \log \left(\frac{\sigma_c}{58 \text{ km s}^{-1}} \right) + (2.20 \pm 0.02), \quad (4)$$

with $\chi^2_r = 1.55$ for LSB galaxies.

Although the uncertainties are large, equations (3) and (4) are consistent with each other well within 1σ, but inconsistent with equation (2) (see also right-hand panel of Fig. 3).

Two interpretations are open at this point. The samples studied to date are far from complete or homogeneous, and it is conceivable that, as more data are collected, more galaxies will fill the gap between the LSB galaxies, which are mainly found in the low-velocity dispersion region, and the extrapolation to low σ_c of equation (2), defined mainly by HSB galaxies. This interpretation allows for the possibility that the log–log v_c–σ_c relation, including both HSB and LSB galaxies, is linear, but that its *scatter* increases going from large to small velocity dispersions. Alternatively, it is possible that the log–log v_c–σ_c relation is not linear, and that indeed its character changes dramatically below $v_c \sim 200$ km s^{-1}, as originally suggested by Ferrarese (2002) and Baes et al. (2003). In either case, it seems unavoidable to conclude that the efficiency of bulge (and, perhaps, SBH) formation is regulated by intrinsic parameters in addition to the depth of the global potential well.

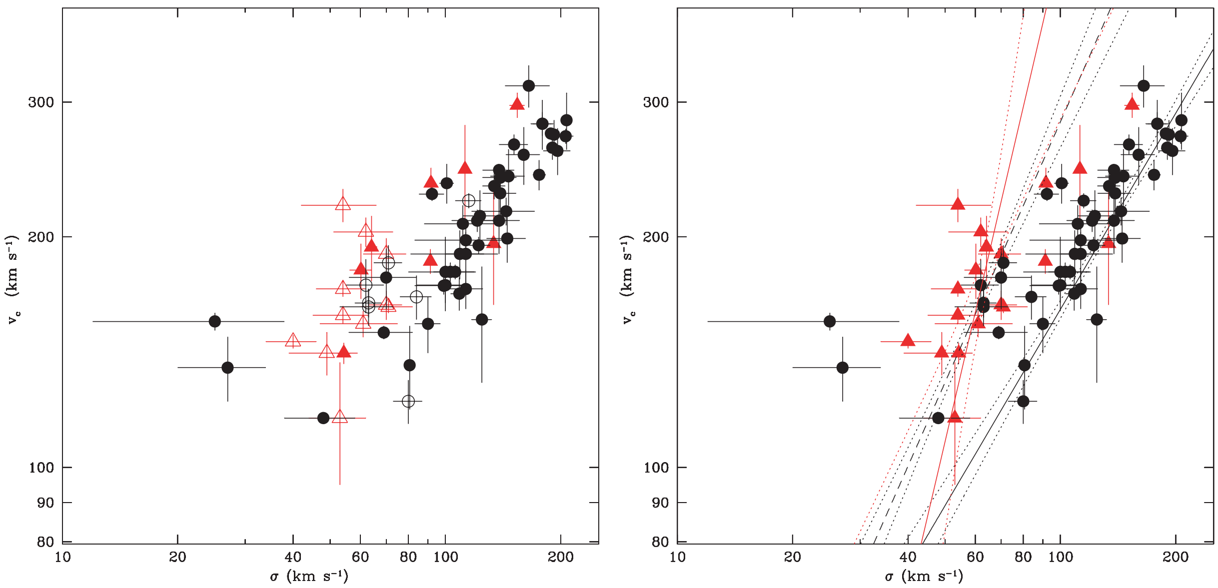

Figure 3. Left-hand panel: the relation between the large-scale disc circular velocity v_c and the central bulge velocity dispersion σ_c for HSBs (black circles) and LSBs (red triangles). Data from Ferrarese (2002), Baes et al. (2003), Pizzella et al. (2005) (full symbols) and this paper (open symbols) are plotted. Right-hand panel: as in the left-hand panel, with fits superimposed. The solid and dashed black lines are least-squares fits to HSB galaxies with $\sigma_c \geqslant 80$ km s^{-1} and $\sigma_c \leqslant 80$ km s^{-1}, respectively. The red solid line is the fit to LSB galaxies with $\sigma_c \leqslant 80$ km s^{-1}. Dotted lines represent the 1σ uncertainties in the fits.

The implications of these findings for the central SBHs cannot be easily quantified. The $M_{\rm BH}-\sigma_c$ relation is not characterized for LSBs, for which no SBH detection has been attempted. It is also not defined below $\sigma_c \leqslant 80$ km s^{-1}, which corresponds to SBHs too small to be detected given current space- or ground-based instrumentation. We reiterate the conclusion of Ferrarese (2002) and Baes et al. (2003) that the behaviour of the $v_c - \sigma_c$ relation at $\sigma_c \lesssim 80$ km s^{-1} might reflect the inability of these galaxies to form a central SBH, as argued on theoretical grounds by, for instance, Shankar et al. (2006); Haehnelt et al. (1998); Silk & Rees (1998); Loeb & Rasio (1994). Numerical simulations (Di Matteo et al. 2003; Robertson et al. 2005) predict that the $M_{\rm BH}$–σ_c relation originates from the feedback between the central SBH and the progenitor of the hot stellar component at the early stages of the formation of both; therefore, in low-mass, late-type HSB and LSB galaxies internal factors might lead to the suppression of such feedback, creating a dynamical relation between disc, bulge and SBH which is starkly different from that displayed by more massive systems.

ACKNOWLEDGMENTS

We thank S. De Rijcke for sharing his software to derive velocity dispersion profiles with us, P. Palunas for providing us the rotational velocities in tabular form and A. Pizzella for the very fruitful discussions. PB wishes to thank the Herzberg Institute of Astrophysics for the hospitality which made this investigation possible. Based on observations made at the European Southern Observatory, Chile (ESO Programme No. 073.B-0780). Based on observations collected at the Centro Astronómico Hispano Alemán (CAHA) at Calar Alto, operated jointly by the Max-Planck Institut für Astronomie and the Instituto de Astrofísica de Andalucía (CSIC). PB acknowledges the Fund for Scientific Research Flanders (FWO) for financial support. This research has made use of the NASA/IPAC Extragalactic Data base (NED) which is operated by the Jet Propulsion Laboratory, California Institute of Technology, under contract with the National Aeronautics and Space Administration.

REFERENCES

Adams F. C., Graff D. S., Richstone D., 2000, ApJ, 551, L31
Baes M., Buyle P., Hau G. K. T., Dejonghe H., 2003, MNRAS, 341, L44
Baggett W. E., Baggett S. M., Anderson K. S. J., 1998, AJ, 116, 1626
Cappellari M., Emsellem E., 2004, PASP, 116, 138
Cattaneo A., Haehnelt M. G., Rees M. J., 1999, MNRAS, 308, 77
Courteau S., 1996, ApJS, 103, 363
De Bruyne V., Vauterin P., De Rijcke S., Dejonghe H., 2003, MNRAS, 339, 215
De Bruyne V., De Rijcke S., Dejonghe H., Zeilinger W. W., 2004, MNRAS, 349, 461
Di Matteo T., Croft R. A. C., Springel V., Hernquist L., 2003, ApJ, 593, 56
Ferrarese L., 2002, ApJ, 578, 90
Ferrarese L., Merritt D., 2000, ApJ, 539, L9
Ferrarese L., Ford H. C., 2005, Space Sci. Rev., 116, 523
Gebhardt K. et al., 2000, ApJ, 539, L13
Ghez A. M., et al., 2003, ApJ, 586, L127
Graham A. W., Erwin P., Caon N., Trujillo I., 2001, ApJ, 563, L11
Haehnelt M. G., Natarajan P., Rees M. J., 1998, MNRAS, 300, 817
Haehnelt M. G., Kauffmann G., 2000, MNRAS, 318, L35
Heraudeau P., Simien F., Mamon G. A., 1996, A&A, 117, 417
Kawakatu N., Saitoh T. R., Wada K., 2005, ApJ, 628, 129
Kormendy J., Richstone D., 1995, ARA&A, 33, 581
Loeb A., Rasio F., 1994, ApJ, 432, L52
Marconi A., Hunt L. K., 2003, ApJ, 589, L21
Miyoshi M., Moran J., Herrnstein J., Greenhill L., Nakai N., Diamond P., Inoue M., 1995, Nat, 373, 127
Möllenhoff C., Heidt J., 2001, A&A, 368, 16
Monaco P., Salucci P., Danese L., 2000, MNRAS, 311, 279
Palunas P., Williams T. B., 2000, AJ, 120, 2884
Pizzella A., Corsini E. M., Dalla Bontá E., Sarzi M., Coccato L., Bertola F., 2005, ApJ, 631, 785
Press W. H., Teukolsky S. A., Vetterling W. T., Flannery B. P., 2002, Numerical Recipes in C++. Cambridge Univ. Press, Cambridge
Robertson B., Hernquist L., Cox T. J., Di Matteo T., Hopkins P. F., Martini P., Springel V., 2005, preprint (astro-ph/0506038)

Schödel R., Ott T., Genzel R., Eckart A., Mouawad N., Alexander T., 2003, ApJ, 596, 1015
Shankar F., Lap A., Salucci P., De Zotti G., Danese L., 2006, ApJ, 643, 14
Silk J., Rees M. J., 1998, A&A, 331, L1
Tremaine S. et al., 2002, ApJ, 574, 740
Verheijen M., 2001, ApJ, 563, 694
Wyithe J. S., Loeb A., 2005, ApJ, 634, 910

This paper has been typeset from a TEX/LATEX file prepared by the author.